Low-Angle Light Scattering from Poly(methyl methacrylate) and Polystyrene–Poly(methyl methacrylate) Mixtures and Blends

H. K. Yuen and J. B. Kinsinger*

Department of Chemistry, Michigan State University, East Lansing, Michigan 48824.
Received November 5, 1973

ABSTRACT: The scattering of light from amorphous poly(methyl methacrylate) and a series of its mixtures and blends with amorphous polystyrene has been studied photometrically as a function of scattering angle using a vertically polarized laser beam. The angular distribution of the scattered intensity has been analyzed with seven different correlation functions suggested by Ross. The evolution of the inhomogeneities and hence morphology with composition is investigated in terms of the correlation function, the short- and long-range correlation distances, the distance of heterogeneity, the volume of heterogeneity, the fractional contribution factor of the short-range correlation function, and the standard deviation in refractive index. The critical weight fraction of polystyrene is determined. It is found that the correlation distances are of macro size and the magnitude of the standard deviation in refractive index increases with the concentration of polystyrene in the blend. The Debye exponential correlation function which characterizes the poly(methyl methacrylate) cannot adequately describe the short-range inhomogeneity in all the mixtures and blends. In accord with the visual opacity of the samples, the experiment also provides quantitative information on the relative compatibility of the blend and mixed systems.

The mechanical and physical properties of solid polymers depend on their degree of inhomogeneity. In the case of solid mixtures such as polyblends, the degree of inhomogeneity also measures relatively the mutual compatibility between the components,[1] that is, the higher the scale of inhomogeneity, the lower the compatibility between the components and *vice versa*.

The usefulness of light scattering for characterizing the inhomogeneity of dimension comparable to the wavelength of the incident light was first suggested for isotropic inhomogeneous solids by Debye and Bueche[2] in 1949. Later, it was extended to systems containing fluctuations in anisotropy by Goldstein-Michalik[3] and Goldstein[4,5] and to crystalline polymers by Stein and his collaborators.[6-8] The isotropic theory of Debye and Bueche has been supplemented by Guinier and Fournet[9] and made more explicitly by Ross.[10] Lately, by examining test specimens of carefully controlled structure, Moritani *et al.*[11] also elucidated the dependence of inhomogeneities on the morphology of blends. Sturgill[12] has shown that, even at a very high volume of a second phase where that phase begins to aggregate, the characteristic scattering intensity associated with independent spherical scatterers remains dominant.

In this paper, we are concerned primarily with the evolution of the inhomogeneity, the morphology plus the compatibility with composition in a series of polystyrene-poly(methyl methacrylate) mixtures and blends. The investigation also includes a sample of pure poly(methyl methacrylate) and is based on the principles of the isotropic theory of light scattering.

Inhomogeneity Characterization

According to Ross,[10] the inhomogeneity in an amorphous solid polymer which is neither magnetic nor conductive may be attributed to the local deviations of the electric permittivity from the mean

$$\delta\epsilon(\mathbf{r}) = \epsilon(\mathbf{r}) - \langle\epsilon\rangle \tag{1}$$

where

$$\langle\epsilon\rangle = \frac{1}{V}\int\int\int_{v} \epsilon(\mathbf{r})dV \tag{2}$$

is the mean permittivity over the volume V of the sample. It is possible to characterize this inhomogeneity by its amplitude and extent. The amplitude is given by the average square of the deviations or variance

$$\langle\delta\epsilon^2\rangle = \frac{1}{V}\int\int\int_{v} [\delta\epsilon(\mathbf{r})]^2 dV \tag{3}$$

whereas the extent is the distance over which the deviation can be regarded as not changing appreciably. To estimate the latter, it is necessary to consider the correlation function of the deviations at any two points situated at a distance ρ apart, namely

$$F(\rho) = \frac{\frac{1}{V}\int\int\int_{v} \delta\epsilon(\mathbf{r})\delta\epsilon(\mathbf{r}+\rho)dV}{\langle\delta\epsilon^2\rangle} \tag{4}$$

As defined, $F(\rho)$ measures the interdependence of the deviations at the two points and takes the following values for $\rho = 0$ and for ρ very large

$$F(0) = 1 \text{ and } \lim_{\rho\to\infty} F(\rho) = 0 \tag{5}$$

The last equation in (5) follows because when the two points are far apart, the deviations will vary independently of one another. Functions such as

$$\begin{aligned} F1 &= \exp(-\rho/a) \\ F2 &= \exp(-\rho^2/a^2) \\ F3 &= 1/[1+(\rho^2/a^2)]^2 \\ F4 &= [(1+\rho/a)]\exp(-\rho/a) \\ F5 &= \exp(-\rho^2/2a^2) \\ F6 &= (\rho/a)K_1(\rho/a) \\ F7 &= \frac{1}{2^{\nu-1}\Gamma(\nu)}(\rho/a)^{\nu}K_{\nu}(\rho/a) \end{aligned} \tag{6}$$

where $K_1(\rho/a)$ and $K\nu(\rho/a)$ are the modified spherical Bessel functions of order 1 and ν, respectively, and $\Gamma(\nu)$ the Gamma function, all satisfy the two basic properties of the correlation function shown in eq 5 and therefore have been suggested for isotropic samples. The parameter a in each of the functions has a dimension of length. It is called the correlation distance and characterizes the *extent* of the inhomogeneity. Thus, a larger value of a signifies a higher degree of inhomogeneity and corresponds to a coarser structure of the sample.

The isotropic theory of light scattering[10] shows that for vertically polarized light of intensity I_0 and wavelength Λ_0

Table I
Thermal History of Pure PMMA and PS–PMMA Samples

Sample	T_1 (°C)	t_1 (hr)	T_2 (°C)	t_2 (hr)	T_3 (°C)	t_3 (hr)	T_4 (°C)	t_4 (hr)	T_5 (°C)	t_5 (hr)
PMMA	40	4	51	14	71	5	101	5		
0.0001% PS–PMMA	45	5	50	14	65	4	80	4	100	21
0.001% PS–PMMA	45	5	50	14	65	4	80	4	100	21
0.005% PS–PMMA	45	5	50	14	65	4	80	4	100	21
0.01% PS–PMMA	45	5	50	14	65	4	80	4	100	21
0.03% PS–PMMA	45	5	50	14	65	4	80	4	100	21
0.05% PS–PMMA	45	5	50	14	65	4	80	4	100	21

incident on an amorphous medium, the scattered intensity $I(s,\beta)$ measured at a point a large distance L away from the sample is proportional to the sine Fourier transform of the correlation function

$$I(s,\beta) = I_0 \frac{V}{L^2} \frac{\langle k\rangle^3}{4\pi} \frac{\langle \delta\epsilon^2\rangle}{\langle\epsilon\rangle^2} \frac{\sin^2\beta}{s} \int_0^\infty \rho F(\rho) \sin(\langle k\rangle \rho s) d\rho \quad (7)$$

where β is the angle between the direction of the electric vector of the incident radiation and the direction of observation, s is related to the scattering angle θ and is equal to 2 sin $(\theta/2)$, V is the illuminated volume, and $\langle k\rangle = (2\pi/\Lambda_0)\langle n\rangle$ is the average wave number of the light in the medium which has a mean refractive index $\langle n\rangle$. If the point of observation is restricted further to lie on the horizontal plane, $\sin^2\beta$ in eq 7 is unity and therefore

$$I(s) = I_0 \frac{V}{L^2} \frac{\langle k\rangle^3}{4\pi} \frac{\langle \delta\epsilon^2\rangle}{\langle\epsilon\rangle^2} \frac{1}{s} \int_0^\infty \rho F(\rho) \sin(\langle k\rangle \rho s) d\rho \quad (8)$$

Thus, by measuring the scattered intensity as a function of the scattering angle, information on the correlation function and, hence, the correlation disstance of the inhomogeneity can be obtained.

For systems containing two components (*e.g.*, polyblends), it has been found[11,13,14] that the angular distribution curve of the scattered intensity sometimes requires a sum of two correlation functions

$$F(\rho) = fF_1 + (1-f)F_2 \quad (9)$$

Here, F_1 is associated with the intensity measured at low angles and is related to the short-range correlation of the domains of the inhomogeneity. F_2, on the other hand, is related to the data obtained at lower angles and measures the long-range correlation between the domains. Accordingly, there are two correlation distances, a_1 and a_2. The first, a_1, is called the short-range correlation distance whereas a_2 is the long-range correlation distance. The parameter f in (9) which statistically weights the contribution of F_1 to $F(\rho)$ is designated as the fractional contribution factor.[11]

Porod[15] in 1951 suggested two more inhomogeneity parameters associated with the correlation function. One is called the distance of heterogeneity, l_c, and is defined by

$$l_c = 2\int_0^\infty F(\rho) d\rho \quad (10)$$

The other is called the volume of heterogeneity, v_c, and is represented by the integral

$$v_c = \int_0^\infty 4\pi\rho^2 F(\rho) d\rho \quad (11)$$

Provided that the two components in a binary system can be regarded as separately homogeneous and have electric permittivities ϵ_1 and ϵ_2, respectively, it can be shown easily that the amplitude of the inhomogeneity or the variance of the permittivity in the sample is given by

$$\langle \delta\epsilon^2\rangle = (\epsilon_1 - \epsilon_2)^2 \phi_1 \phi_2 \quad (12)$$

Table II
Dimensions and Mean Refractive Indices of Pure PMMA and PS–PMMA Samples

Sample	Diameter (cm)	Length (cm)	$\langle n\rangle_{5145}$
PMMA	1.585	1.915	1.4942
0.0001% PS–PMMA	1.595	1.910	1.4943
0.001% PS–PMMA	1.585	1.946	1.4943
0.005% PS–PMMA	1.593	1.923	1.4944
0.01% PS–PMMA	1.590	1.895	1.4946
0.03% PS–PMMA	1.582	1.930	1.4947
0.05% PS–PMMA	1.590	1.913	1.4948

Here, ϕ_1 and ϕ_2 are the volume fractions of the two components. In the case of polyblend where the second polymer is distributed in a matrix formed by the first, eq 12 shows that if $\phi_1 > \phi_2$ and if the two polymers have about the same density, the amplitude of the inhomogeneity increases with respect to the concentration of the second component. In practice, it is more convenient to measure refractive index than electric permittivity. Making use of the Maxwell formula, $\epsilon = n^2$, it can be shown that

$$\frac{\langle \delta\epsilon^2\rangle}{\langle\epsilon\rangle^2} \simeq \frac{4\langle(\delta n)^2\rangle}{\langle n\rangle^2} \quad (13)$$

if the deviations in refractive index, $\delta n(\mathbf{r})$, about the mean, $\langle n\rangle$, are small. Information on the amplitude of the inhomogeneity can be obtained by measuring the turbidity, τ, of the sample.[10] By definition, the turbidity is the scattering cross section over all directions

$$\tau = \iint \frac{I(s,\beta)L^2}{I_0 V} d\Omega = \int_0^\pi \int_0^{2\pi} \frac{I(s,\beta)L^2}{I_0 V} \sin\theta d\psi d\theta \quad (14)$$

where β, as defined previously, is the angle between the electric vector of the incident radiation and the direction of observation. Substituting eq 7 into eq 14 and realizing that $\sin^2\beta = 1 - \sin^2\theta \sin^2\psi$, where θ is the scattering angle (in this case, the polar angle) and ψ the azimuthal angle, one obtains after integrating over ψ, changing the variable θ to s according to $s = 2 \sin(\theta/2)$ and taking eq 13 into account

$$\tau = 2\langle k\rangle^3 \frac{\langle \delta n^2\rangle}{\langle n\rangle^2} \left\{ \int_0^2 \left[\int_0^\infty \rho F(\rho) \sin(\langle k\rangle \rho s) d\rho \right] ds - \frac{1}{8}\int_0^2 (4s^2 - s^4) \left[\int_0^\infty \rho F(\rho) \sin(\langle k\rangle \rho s) d\rho \right] ds \right\} \quad (15)$$

Thus, by determining the correlation function, $F(\rho)$, from the angular distribution of the scattered intensity and measuring the turbidity of the sample, the standard deviation in refractive index, $(\langle \delta n^2\rangle)^{1/2}$, can be calculated.

Experimental Section

Sample Preparation. The materials used to prepare the samples consisted of stabilized methyl methacrylate monomer, narrow molecular weight distribution polystyrene and α,α'-azobis(isobutyronitrile) (AIBN) initiator. The monomer was obtained

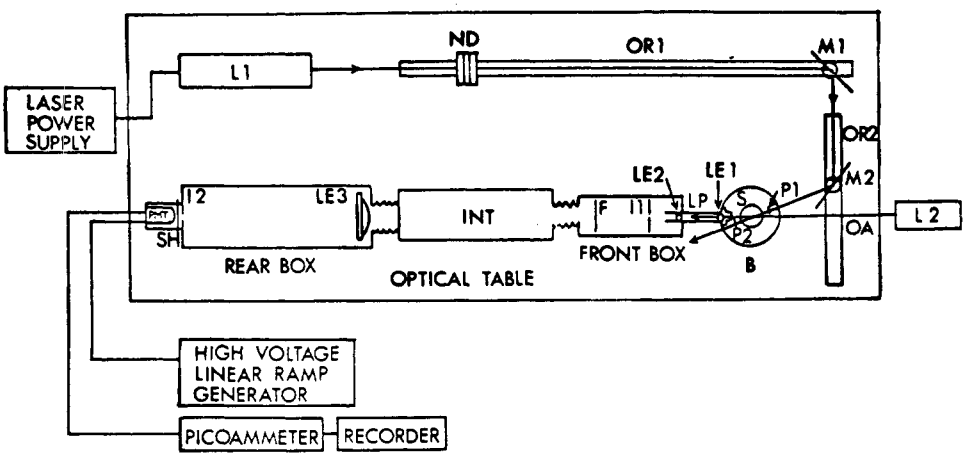

L1 = Argon Ion Laser
ND = Neutral Density Filters
OR1 = Optical Rail 1
M1 = Mirror 1
OR2 = Optical Rail 2
M2 = Mirror 2
L2 = He-Ne Alignment laser
OA = Optical Axis
P1 = Alignment Pinhole 1
S = Sample Holder
P2 = Alignment Pinhole 2

B = Bridgeport Table
LE1 = Small Light Pipe Lens 1
LP = Light Pipe
LE2 = Small Light Pipe Lens 2
I1 = Large Iris Diaphragm 1
F = Gelatin Green Filter
INT = Empty Fabry Perot Interferometer Housing
LE3 = Focussing Lens (f = 500 mm)
I2 = Large Iris Diaphragm 2
SH = Photographic Shutter

Figure 1. Schematic drawing of the low-angle photometer.

from the Eastman Kodak Co. which also supplied the AIBN initiator. The polystyrene was of the anionically polymerized type (mol wt 82,500) and was kindly supplied by the Dow Chemical Co. Before use, the monomer was carefully freed from its hydroquinone stabilizer with aliquots of 5% sodium hydroxide solution and was distilled under 100 mm. Only the middle portion of the distillate whose purity had been checked with gas chromatography was collected and employed in the preparation. The AIBN initiator was also purified by recrystallization over Spectrograde benzene.

Altogether seven samples ranging from a pure poly(methyl methacrylate) (PMMA) and six mixtures and blends of 0.0001, 0.001, 0.005, 0.01, 0.03, and 0.05% by weight of polystyrene (PS) in poly(methyl methacrylate) were prepared with about 0.1% of the AIBN initiator. The amount of polystyrene used for the 0.001 and 0.0001% mixtures were obtained by successive dilution of the 0.005% polymer–monomer solution with monomer. All glassware was rigorously cleaned by the conventional procedures for high quality light-scattering samples. Solutions of the monomer–initiator and polymer–monomer–initiator were filtered respectively through a combination of a very fine sintered-glass filter, a 0.25 μ Millipore filter and an ultrafine sintered-glass filter into cylindrical Pyrex sample tubes where they were degassed by the standard freeze–thaw method and were finally sealed under vacuum. The polymerization of the monomer was achieved thermally at 50° and was completed at an annealing temperature of 100°. Since the inhomogeneity in a sample may be affected by its thermal history, the mixtures and blends were all subjected to the same heat treatment. Table I shows the thermal history of our seven samples.

After polymerization and removal from the glass tubes, each sample was cut into two portions. One portion was machined in a lathe into a perfect cylinder with two flat ends, while the other portion was milled into a rectangular tile (2 × 1.5 × 0.5 cm^3). The curved surface of the cylindrical portion was polished carefully in the lathe first with super fine emery paper and then with "Semichrome" Plexiglas polish (product of Competition Chemical Co., Iowa). The flat surfaces of the two portions of the sample were similarly polished but on a flat table. To preserve the thermal history of the sample, liquid nitrogen cooling was applied during the machining and the polishing processes. The polished samples were extremely smooth and were almost free from scratches or surface blemishes. The interiors were completely free from bubbles and visible defects. The cylindrical portions were used for light scattering and the rectangular tiles were used for refractive index measurements which were performed on a Bausch & Lomb-3L refractometer. Table II shows the dimensions of the polished cylindrical samples and their mean refractive indices at the wavelength of the light (Λ_0 = 5145 Å) used in the scattering experiment.

Low-Angle Photometer. The photometer used to measure the scattered radiation at low angles (Figure 1) was a modified Brillouin spectrometer without the Fabry–Perot interferometer. It was originally designed by Gaumer[16] and was constructed on a vibration-free optical table.

The optical source was furnished by a Spectra Physics 165 Argon ion single mode laser which could be tuned to deliver a frequency stabilized and vertically polarized green line of wavelength 5145 Å. The light was first attenuated by a series of neutral density filters and then reflected by two high quality mirrors carried on two separated but perpendicular optical rails into an open sample compartment.

The sample compartment consisted of a pair of interlocked pinholes of 1 mm in diameter situated on either side of a 2 in. × 2 in. sample holder bracket which was placed at dead center on a Bridgeport rotary table. The two pinholes which had been lined up initially with the optical axis of the photometer with a small He–Ne laser served as reference standards for the incident beam. Since the detection system of the photometer was fixed in position, scattering angles from 3 to 135° could be obtained from the Bridgeport table scales to an accuracy of five seconds of a degree.

The scattered radiation from the sample was first collected by a 18-in. long light pipe[17] which had a small conical nose piece in front carrying a rectangular slit of 0.004 in. in width and 0.04 in. in length. Diffraction from the slit was eliminated by two small lenses (f = 50 and 136 mm, respectively) inside the pipe which focused the light to a large iris diaphragm adjusted to pass only the image of the slit. The light pipe assembly provided a resolution angle no larger than 0.6° on the horizontal plane. From the baffle iris, the scattered light was first probed by a Kodak wratten gelatin green filter whereby any components due to fluorescence were removed. Then, the light propagated through an empty Fabry–Perot interferometer housing and was finally focused by a large achromatic lens of f = 500 mm into a photomultiplier tube (EMI 9558B) which was protected in front by another baffle iris diaphragm. The photomultiplier tube was housed in a refrigerated chamber. The signal from the photomultiplier was amplified by a Keithley 417 picoammeter and was recorded on a Sargent recorder.

Scattered Intensity Measurements. The sample in its holder[17] was placed into the square bracket on the Bridgeport table of the photometer such that the incident beam (Λ_0 = 5145 Å) was normal to one of its flat surfaces. The intensity of the scattered radiation emerging from the other flat end of the sample was measured relatively at room temperature as a function of the scattering angle and was then corrected for the effects due to re-

Table III
Power Spectrum and Turbidity Expressions for Seven Types of Correlation Functions

$F(\rho)$	$I(s)$	τ
$F1 = \exp(-\rho/a)$	$A\frac{1}{\pi}\frac{q^3}{(4+q^2s^2)^2}$	$\langle k\rangle\frac{\langle\delta n^2\rangle}{\langle n\rangle^2}\left\{q\left[\frac{(q^2+2)^2}{q^2(1+q^2)}-\frac{2q^2+2}{q^4}\ln(1+q^2)\right]\right\}$
$F2 = \exp[-(\rho/a)^2]$	$A\frac{1}{128\sqrt{\pi}}q^3\exp\left(-\frac{q^2s^2}{16}\right)$	$\langle k\rangle\frac{\langle\delta n^2\rangle}{\langle n\rangle^2}\left\{\frac{\sqrt{\pi}}{2}q\left[\left(1+\frac{64}{q^4}\right)[1-\exp(-q^2/4)]-\frac{8}{q^2}[1+\exp(-q^2/4)]\right]\right\}$
$F3 = 1/[1+(\rho/a)^2]^2$	$A\frac{1}{128}q^3\exp(-qs/2)$	$\langle k\rangle\frac{\langle\delta n^2\rangle}{\langle n\rangle^2}\left\{\frac{\pi}{4}q\left[1-\frac{12}{q^2}+\frac{240}{q^4}-\left(q+5+\frac{28}{q}+\frac{108}{q^2}+\frac{240}{q^3}+\frac{240}{q^4}\right)\exp(-q)\right]\right\}$
$F4 = (1+\rho/a)\exp(-\rho/a)$	$A\frac{16}{\pi}\frac{q^3}{(4+q^2s^2)^3}$	$\langle k\rangle\frac{\langle\delta n^2\rangle}{\langle n\rangle^2}\left\{2q\left[\frac{(q^4-2q^2-2)(2+q^2)}{q^2(1+q^2)^2}+\frac{4}{q^4}\ln(1+q^2)\right]\right\}$
$F5 = \exp[-(\rho/a)^2/2]$	$A\frac{1}{32\sqrt{2}\sqrt{\pi}}q^3\exp\left(-\frac{q^2s^2}{8}\right)$	$\langle k\rangle\frac{\langle\delta n^2\rangle}{\langle n\rangle^2}\left\{\frac{\sqrt{\pi}}{\sqrt{2}}q\left[\left(1+\frac{16}{q^4}\right)[1-\exp(-q^2/2)]-\frac{4}{q^2}[1+\exp(-q^2/2)]\right]\right\}$
$F6 = (\rho/a)K_1(\rho/a)$	$A\frac{3}{2}\frac{q^3}{(4+q^2s^2)^{5/2}}$	$\langle k\rangle\frac{\langle\delta n^2\rangle}{\langle n\rangle^2}\left\{\frac{3\pi}{2}q\left[\frac{\sqrt{(1+q^2)^3}-1}{3\sqrt{(1+q^2)^3}}\frac{q^4+2q^2+2}{q^4}-2\frac{\sqrt{(1+q^2)}-1}{\sqrt{(1+q^2)}}\frac{q^2+2}{q^4}-2\frac{1-\sqrt{(1+q^2)}}{q^4}\right]\right\}$
$F7 = \frac{1}{2^{\nu-1}\Gamma(\nu)}(\rho/a)^\nu K_\nu(\rho/a)$	$A\frac{2^{2\nu}}{2\sqrt{\pi}}\frac{\Gamma[\nu+(3/2)]}{\Gamma(\nu)}\frac{q^3}{(4+q^2s^2)^{\nu+3/2}}$	$\langle k\rangle\frac{\langle\delta n^2\rangle}{\langle n\rangle^2}\left\{\sqrt{\pi}\frac{\Gamma[\nu+3/2)]}{\Gamma(\nu)}q\left[\frac{(1+q^2)^{\nu+1/2}-1}{[\nu+(1/2)](1+q^2)^{\nu+1/2}}\frac{q^4+2q^2-2}{q^4}-2\frac{(1-q^2)^{\nu-1/2}-1}{[\nu-(1/2)](1+q^2)^{\nu-1/2}}\frac{q^2+2}{q^4}+2\frac{(1+q^2)^{\nu-3/2}-1}{[\nu-(3/2)](1+q^2)^{\nu-3/2}}\frac{1}{q^4}\right]\right\}$

$A = (I_0V/L^2)\langle k\rangle\langle(\delta\epsilon^2)/\langle\epsilon\rangle^2\rangle$; $q = 2\langle k\rangle a$; $s = 2\sin(\theta/2)$.

fraction, reflection and scattering volume (also attenuation for the 0.03 and 0.05% PS-PMMA blends).[17] The scattering angle was also corrected for refraction inside the sample.[17]

Turbidity Measurements. For convenience and better reproducibility, the turbidity of the sample, τ, was determined with the neutral density filters placed between the large f = 500-mm lens and the exit iris diaphragm in front of the photomultiplier tube. Two intensity measurements were made at 0° setting of the Bridgeport table for the incident beam: (1) with no sample in its path and (2) after it transversed through a sample of length l. The latter intensity was further corrected for the effect due to reflection from the interfaces of the sample.[17] The results were $I(0)$ and $I(l)$, respectively. The turbidity of the sample was then calculated from the Lambert equation

$$\tau = (1/l)[\ln I(0) - \ln I(l)] \tag{16}$$

Data Analysis

Although, from eq 8, the correlation function $F(\rho)$ is seen to be obtainable in principle from the Fourier transform of the scattered intensity, it has been suggested by Debye[2] and Ross[14] that in practice a more convenient method is to find an analytical expression whose corresponding power spectrum matches the experimental intensity distribution function.

Among the seven types of correlation functions shown in eq 6, $F1$ and $F2$ are the most common.[2,11,13,18-21] For experiments whose angular distribution of scattered intensity requires two expressions for the correlation function (eq 9), F2[11,13,14,22,23] has always been suggested and found in agreement with the lower angle portion of the distribution. Opinions on the type of correlation function for the low-angle portion are, however, not unanimous. Although $F1 = \exp(-\rho/a)$ which was first proposed by Debye and Bueche[2] is still the most popular, great controversy[10] exists about its physical validity because (1) it is related to a completely disordered structure or a Markov process and (2) its derivative is discontinuous at the origin. For this reason, in the present study, all seven types of correlation functions were tested and wherever necessary $F2 = \exp(-\rho^2/a^2)$ was added to account for the lower angle portion of the scattered intensity distribution.

Table III lists the expressions of the corresponding power spectrum $I(s)$, and turbidity, τ, of each of the seven types of correlation functions as calculated from eq 8 and 15 respectively. There, a dimensionless quantity

$$q = 2\langle k\rangle a \tag{17}$$

has been used instead of the correlation distance a and A is represented by $(I_0V/L^2)\langle k\rangle\langle(\delta\epsilon^2)/\langle\epsilon\rangle^2\rangle$. The power spectrum expressions can be rearranged to the forms shown in the second column of Table IV. Hence, if the experimentally measured intensity, $I(s)$, is plotted according to the scheme shown in the third column of the same table, a straight line will result for the correct correlation function.

The numerical analysis was performed with a CDC 6500 computer. Before the computer fit and in order to determine if the angular distribution of the scattered intensity could be characterized by a single correlation function, the scattering data of each sample were plotted with $I(s)$ *vs.* s according to the scheme shown in the third column of Table IV for each type of correlation function. It was found that except for the pure PMMA sample, the data of all the PS-PMMA mixtures and blends needed to be characterized by a sum of two correlation functions as shown in eq 9.

The low-angle data (with PMMA, all data) were first fitted nonlinearly with each of the power spectrum expressions shown in Table III, whereby the correct correlation function, F_1 (eq 9), was established by comparing the

Table IV
Linear-Fit Equations and Graphing Schemes

$F(\rho)$	Linear-Fit Equation	Plotting Scheme	q	A
$F1 = \exp(-\rho/a)$	$I^{-1/2}(s) = U(1) + U(2)s^2$	$I^{-1/2}$ *vs.* s^2	$2\left[\frac{U(2)}{U(1)}\right]^{1/2}$	$\frac{16\pi}{[U(1)]^2q^3}$
$F2 = \exp[(-\rho/a)^2]$	$\ln I(s) = U(1) - U(2)s^2$	$\ln I$ *vs.* s^2	$4[U(2)]^{1/2}$	$\frac{128\sqrt{\pi}}{q^3}\exp[U(1)]$
$F3 = 1/[1 + (\rho/a)^2]^2$	$\ln I(s) = U(1) - U(2)s$	$\ln I$ *vs.* s	$2U(2)$	$\frac{128}{q^3}\exp[U(1)]$
$F4 = (1 + \rho/a)\exp(-\rho/a)$	$I^{-1/3}(s) = U(1) + U(2)s^2$	$I^{-1/3}$ *vs.* s^2	$2\left[\frac{U(2)}{U(1)}\right]^{1/2}$	$\frac{4\pi}{[U(1)]^3q^3}$
$F5 = \exp[-(\rho/a)^2/2]$	$\ln I(s) = U(1) - U(2)s^2$	$\ln I$ *vs.* s^2	$2[2U(2)]^{1/2}$	$\frac{32\sqrt{2}\sqrt{\pi}}{q^3}\exp[U(1)]$
$F6 = (\rho/a)K_1(\rho/a)$	$I^{-2/5}(s) = U(1) + U(2)s^2$	$I^{-2/5}$ *vs.* s^2	$2\left[\frac{U(2)}{U(1)}\right]^{1/2}$	$\frac{64}{3[U(1)]^{5/2}q^3}$
$F7 = \frac{1}{2^{\nu-1}\Gamma(\nu)}(\rho/a)^\nu K_\nu(\rho/a)$	$I^{-1/(\nu+3/2)}(s) = U(1) + U(2)s^2$	$I^{-1/(\nu+3/2)}$ *vs.* s^2	$2\left[\frac{U(2)}{U(1)}\right]^{1/2}$	$\frac{4^{\nu+3/2}[2\sqrt{\pi}\Gamma(\nu)]}{2^{2\nu}\Gamma[\nu + (3/2)][U(1)]^{\nu+3/2}q^3}$

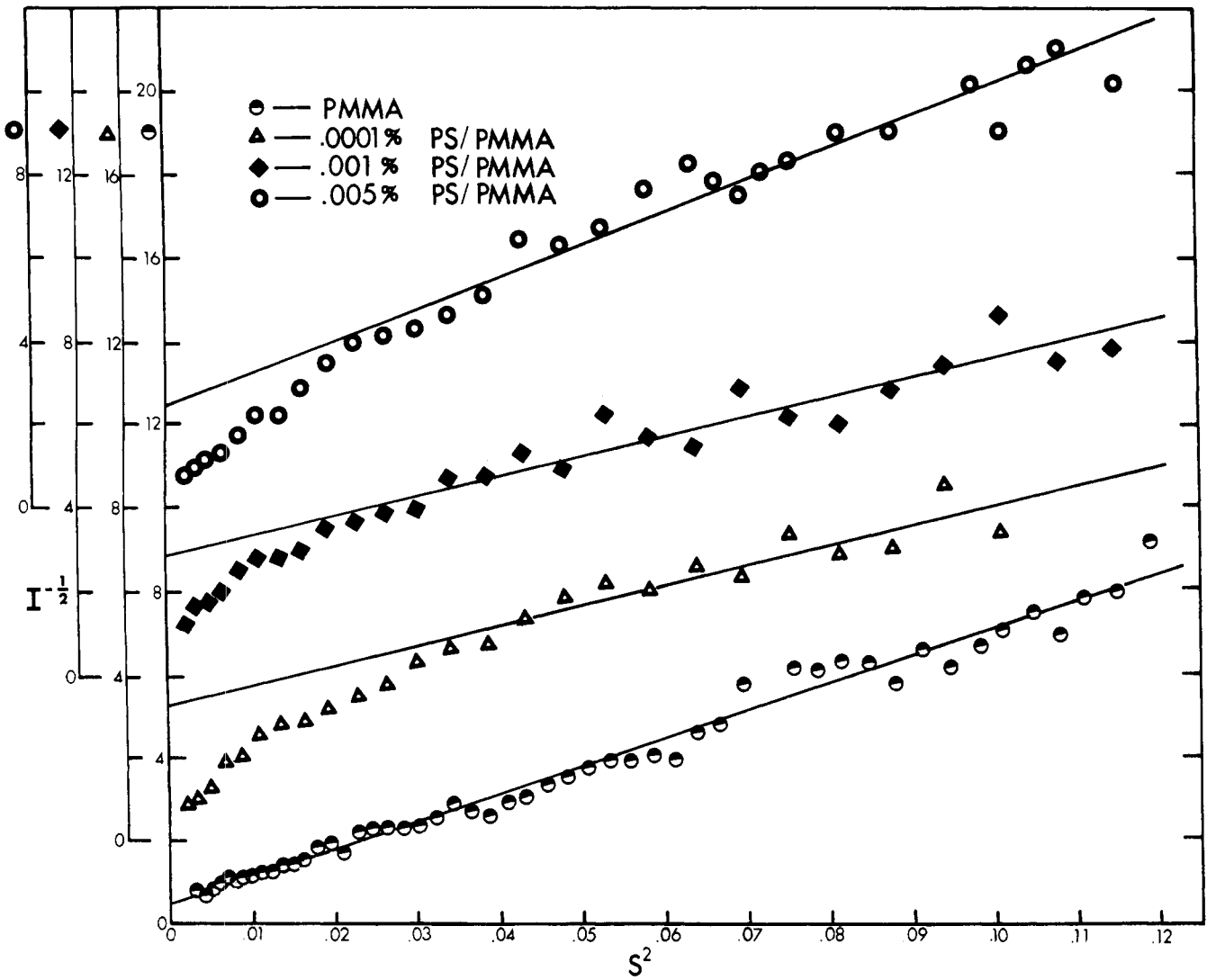

Figure 2. Distribution on the scattered intensity at low angles: plot of $I^{-1/2}$ *vs.* s^2 for PMMA, 0.0001, 0.001, and 0.005% PS-PMMA samples.

sum of the square of the residual (residual = $I(s)_{cal} - I(s)_{exp}$) in each case. The function was then checked by least-square fitting the data against the linear counterpart of its power spectrum outlined in the second column of Table IV. The data are shown in Figures 2 and 3 for the seven samples under study. From these graphs and with reference to the fourth and fifth columns of Table IV, the associated parameters q_1 and A_1 were calculated.

To treat the lower angle data, the difference between the observed scattered intensity and that calculated from the power spectrum expression just established for the low angles was first computed. The resultant data were then

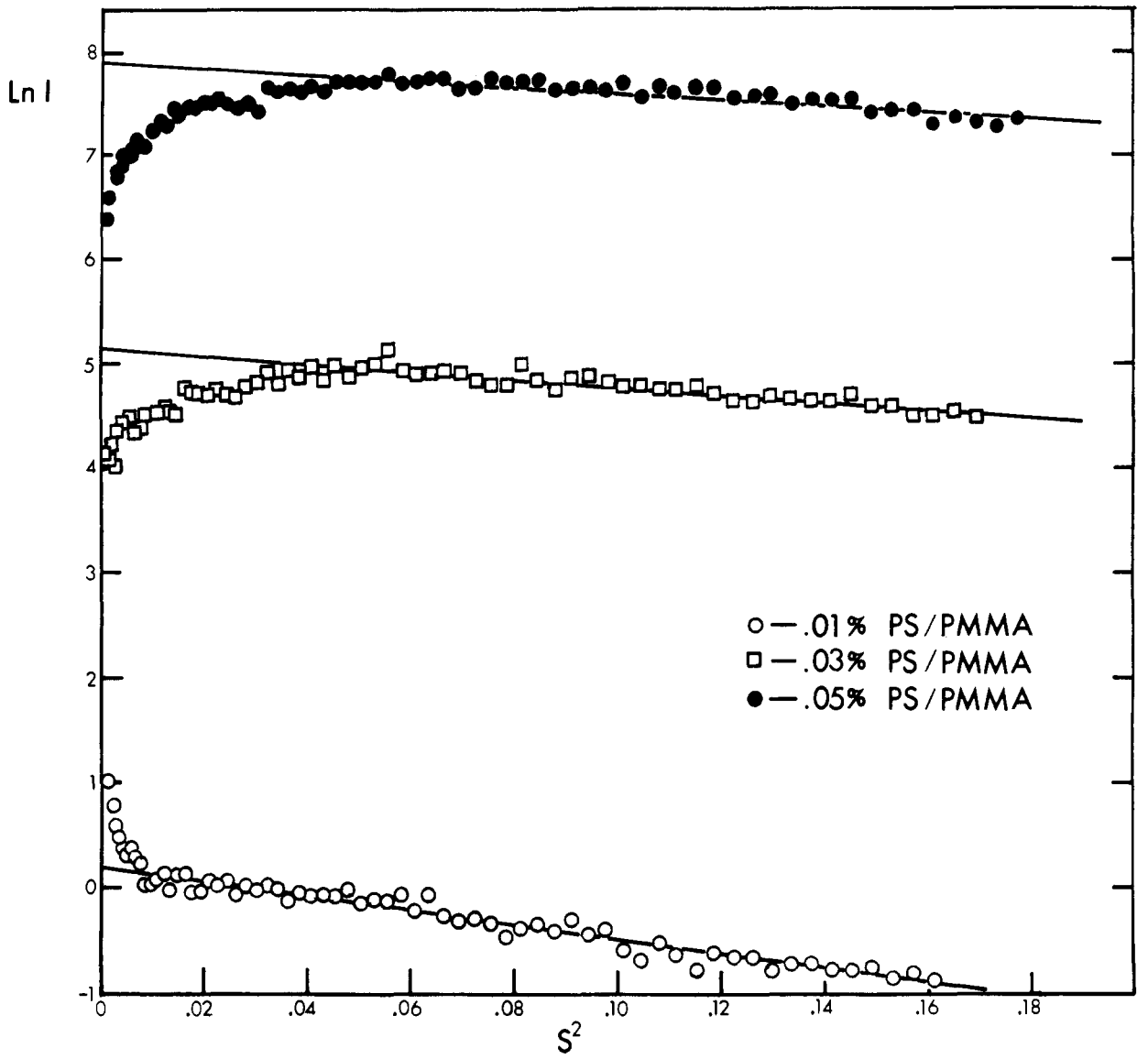

Figure 3. Distribution of the scattered intensity at low angles: plot of ln I *vs.* s^2 for 0.01, 0.03, and 0.05% PS-PMMA samples.

fitted linearly with $F2$ according to the equation shown in the second column of Table IV. Figure 4 shows the graphs so obtained for the mixtures and blend ranging from 0.0001 to 0.01% in polystyrene. From the graphs, the parameters q_2 (hence, the long-range correlation distance a_2) and A_2 were determined in the same way as described for q_1 and A_1.

From eq 9 and 8, it follows that $A_1 = fA$ and $A_2 = (1 - f)A$, where f is the fractional contribution factor and A, as defined before, is $(I_0V/L^2)\langle k\rangle(\langle\delta\epsilon^2\rangle/\langle\epsilon\rangle^2)$. Thus, f was evaluated from A_1 and A_2 by the following equation: $f = A_1/(A_1 + A_2)$.

With the knowledge of a_1, a_2, f and the correlation function $F(\rho)$, the distance of heterogeneity l_c and the volume of heterogeneity v_c were calculated from eq 10 and 11, respectively. Having also measured the turbidity τ and taken into account eq 9, the standard deviation of the refractive index of the sample, $(\langle\delta n^2\rangle)^{1/2}$, was obtained from the expressions shown in the third column of Table III.

Table V summarizes the results obtained for each of the seven samples under study.

Discussion

As previously noted, if the scattered intensity $I(S)$ is plotted against the scattering angle according to the schemes presented in the third column of Table IV, a straight line should obtain for the correct correlation function; however, this linear condition is only partially satisfied by our data. A sinusoidal nature of the data is especially noticeable in Figure 2, 3, and 4. We attribute this variation to a component of the scattered light which derives from speckle clearly seen in the sample. Ross[24] has suggested that highly spatially coherent radiation from a laser source is less suitable for scattering measurements in inhomogeneous media than the less coherent light from a mercury source because of an additional component due to speckle. A similar sinusoidal character is also present in the data of Moritani.[11] Through his elegant sample preparation and coordinated electron micrograph studies, Moritani showed a one-to-one correspondence between the dimensions calculated from his correlation distance (a_1) and those measured from the electron micrographs. It is apparent that an average over the sinusoidal variation does not affect the correlation distance significantly; however, it does contribute to the standard deviation of the numerical fit of the data. The structural information contained in the speckle has not been researched and reported in the literature. We were unable to obtain a_2 values for two of the blends because of multiple scattering and interparticle destructive interference.[25]

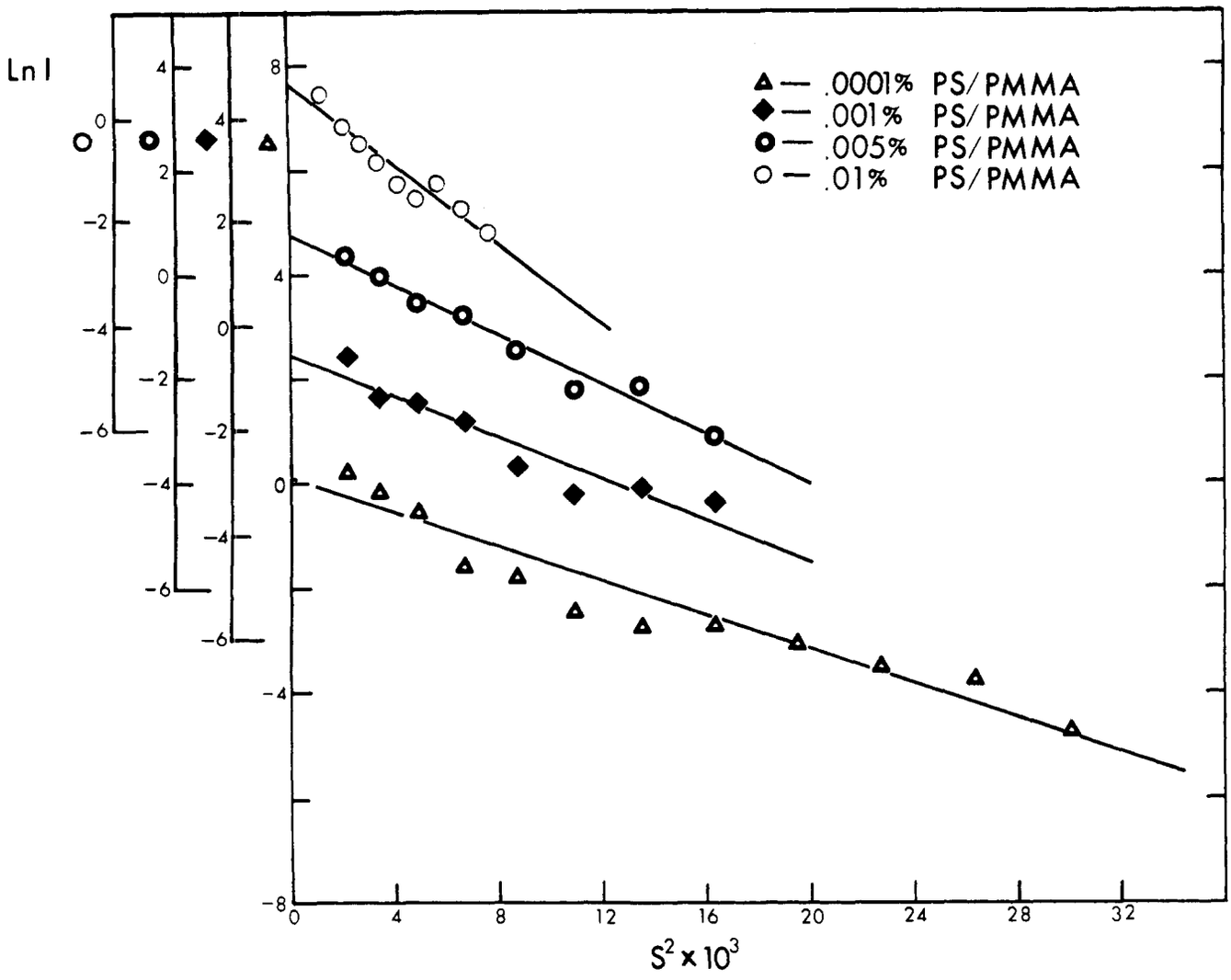

Figure 4. Distribution of the scattered intensity at lower angles: plot of ln I *vs.* s^2 for 0.0001, 0.001, 0.005, and 0.01% PS–PMMA samples.

Our samples (Table V) constitute both mixtures and blends of two polymers along with sample I which is pure PMMA. We have a set of amorphous mixtures with a concentration increasing toward the critical value (samples I, II, III, and IV). Between samples IV and V the critical concentration is reached and the subsequent three samples (V, VI, and VII) are much more opaque and scatter considerably more light. Sample IV is very close to the critical concentration and may represent an amorphous system with "frozen in" critical concentration fluctuations.

Of the seven correlation functions tested, the simple exponential ($F1$) proposed by Debye many years ago fits the low angle data of four of the seven samples best. The lower angle data was represented well with the gaussian correlation function $F2$.

Comparing the values of a_1 and a_2 for the first three mixtures (see columns 5 and 6 of Table V), it is seen that the extent of inhomogeneity increases steadily with concentration. This signifies a decrease in compatibility as more polystyrene is present in the poly(methyl methacrylate) matrix. The increase in the two parameters may be attributed to a size enlargement of the polystyrene domain[11] which results from the larger concentration and the poorer affinity with the matrix. The diminution in the fractional contribution factor f with the 0.005% mixture (see column 7 of Table V) reflects a more pronounced concentration fluctuation in the sample. This suggests that the concentration of polystyrene in the mixture is approaching the critical value. The sudden decrease[26] in the a_1 value in sample V is attributed to phase separation of the polystyrene particles, a process which is always accompanied by a decrease in size. Furthermore, the value of f being so close to unity implies a uniform dispersion of the particles in the sample which also accounts for the increase in the long-range correlation distance a_2.[11] The values of the short-range correlation distance a_1 for the 0.03 and 0.05% blends are smaller than that for the 0.01% sample. Hence the separated polystyrene phase becomes richer in polystyrene.

Mixtures containing 0.005% polystyrene or less are transparent, while blends containing more than 0.01% are opaque. This fact, in conjunction with the changes in the short- and long-range correlation distances (a_1 and a_2) at the 0.01% polystyrene level just discussed, suggests that the former mixtures are compatible while blends containing 0.01% or more of polystyrene have undergone phase separation and are therefore incompatible.

Taking into account eq 9, it can be seen from eq 10 and 11 that the distance of heterogeneity l_c and the volume of heterogeneity v_c are strongly dependent on the value of the fractional contribution factor f. That is, the smaller the value of f, the larger are the parameters. This is illustrated in the eighth and ninth columns of Table V.

The turbidity and the standard deviation of the refractive index of each of the samples under study are shown in

Table V
Inhomogeneity Parameters for Pure PMMA and PS–PMMA Mixtures and Blends

	Sample	$F(\rho)$[a]	q_1	q_2	a_1 (Å)	a_2 (μ)	f	l_c (Å)[b]	v_c (μ^3)[b]	τ (cm^{-1})	$\sqrt{\langle\delta n^2\rangle} \times 10^4$[b]
I	PMMA	$F1$	23.1		6330			12,700	6.37	0.00551	0.545
II	0.0001% PS–PMMA	$fF1 + (1-f)F2$	7.62	50.0	2090	1.37	0.867	6,850	2.10	0.0192	1.41 [1.05][d]
III	0.001% PS–PMMA	$fF1 + (1-f)F2$	8.13	56.0	2230	1.53	0.939	5,840	1.48	0.0326	2.00 [3.31][d]
IV	0.005% PS–PMMA	$fF1 + (1-f)F2$	11.2	61.6	3070	1.69	0.742	12,300	7.47	0.0750	2.05 [7.41][d]
V[c]	0.01% PS–PMMA	$fF2' + (1-f)F2$	10.3	78.4	2820	2.15	0.996	5,130	0.346	0.111	3.94 [10.5][d]
VI[c]	0.03% PS–PMMA	$F2'$	7.56		2070			(3,670)	(0.0494)	1.08	(15.0) [18.2][d]
VII[c]	0.05% PS–PMMA	$F2'$	6.83		1870			(3,310)	(0.0364)	2.32	(23.4) [23.4][d]

[a] $F1 = \exp(-\rho/a_1)$; $F2' = \exp[-(\rho/a_1)^2]$; $F2 = \exp[-(\rho/a_2)^2]$. [b] Numbers in parentheses are calculated by assuming $f = 1$. [c] Samples with phase separation. [d] Calculated from eq 19.

columns 10 and 11 of Table V, respectively. The turbidity of our PMMA sample is smaller than that reported by Debye and Bueche[2] for *commercial* Lucite (9.53×10^{-3} cm^{-1} for blue light of $\Lambda_0 = 4358$ Å or 6.78×10^{-3} cm^{-1} for $\Lambda_0 = 5145$ Å). This indicates the higher level of purity of our sample. Among the mixtures and blends, the standard deviation of the refractive index is seen to increase with the concentration of polystyrene. In order to determine how well this increase in the amplitude of the inhomogeneity can be interpreted in terms of the refractive indices of the two phases and their concentration, eq 12 is rewritten as follows

$$\langle\delta n^2\rangle = (n_1 - n_2)^2\phi_1\phi_2 \tag{18}$$

where n_1 and n_2 are the refractive indices of pure poly(methyl methacrylate) and polystyrene, respectively, and ϕ_1 and ϕ_2, their volume fractions. As the density[27] of the two amorphous polymers is about the same ($\rho_{PMMA} = 1.17$, $\rho_{PS} = 1.05$), eq 18 can also be expressed in terms of their weight fractions, w_1 and w_2

$$\langle\delta n^2\rangle = (n_1 - n_2)^2 w_1 w_2 \tag{19}$$

The numbers in brackets in column 11 of Table V are calculated from eq 19 where the refractive index of polystyrene[28] at the wavelength of 5145 Å is taken to be 1.599. It is seen that the experimental values of the standard deviation of the refractive index agree with those calculated except near the critical concentration for phase separation. The agreement is particularly good at the highest polystyrene content where the two separated phases of the sample are pure.

Conclusions

The inhomogeneity in pure amorphous PMMA and its mixtures and blends with various concentrations of polystyrene, subject to an identical thermal history, have been characterized by studying the angular distribution of the scattered light intensity. The following conclusions are made. (1) The simple exponential correlation function of Debye and Bueche associates only with pure PMMA and at low angles, with mixtures containing respectively 0.0001 and 0.001, and 0.005% of polystyrene. At and above a concentration of 0.01%, however, the blends require a more complex correlation function of the gaussian type. (2) Both the short (a_1) and long-range correlation distances (a_2) are of macro size. The latter is much larger than the former being in the region of a micron. (3) The compatibility of the mixtures and blends decreases with higher concentration of polystyrene. (4) A trend of behavior opposite to that of the compatibility is observed for the standard deviation of the refractive index in the mixtures and blends. (5) We find the critical turbidity of PS in PMMA to be $\tau_c = 0.09$ cm^{-1} and the critical concentration $C_c = 0.008$ wt % polystyrene.

References and Notes

(1) A. J. Yu, *Advan. Chem. Ser.*, **99**, 2 (1971).
(2) P. Debye and A. M. Bueche, *J. Appl. Phys.*, **20**, 518 (1949).
(3) M. Goldstein and E. R. Michalik, *J. Appl. Phys.*, **26**, 1450 (1955).
(4) M. Goldstein, *J. Appl. Phys.*, **30**, 493, 501 (1959).
(5) M. Goldstein, *J. Appl. Phys.*, **33**, 3377 (1962).
(6) R. S. Stein and M. B. Rhodes, *J. Appl. Phys.*, **31**, 1873 (1960).
(7) R. S. Stein and P. R. Wilson, *J. Appl. Phys.*, **33**, 1914 (1962).
(8) R. S. Stein, P. R. Wilson, and S. N. Stidham, *J. Appl. Phys.*, **34**, 46 (1963).
(9) A. Guinier and G. Fournet, "Small-Angle Scattering of X-rays," Wiley, New York, N. Y., 1955.
(10) G. Ross, *Opt. Acta*, **15**, 451 (1968).
(11) M. Moritani, T. Inoue, M. Motegi, and H. Kawai, *Macromolecules*, **3**, 433 (1970).
(12) D. T. Sturgill, *Amer. Ceramic Soc. Spec. Publ. No. 5* (1972).
(13) P. Debye, H. R. Anderson, Jr., and H. Brumberger, *J. Appl. Phys.*, **28**, 679 (1957).
(14) G. Ross, *Opt. Acta*, **16**, 95 (1969).
(15) G. Porod, *Kolloid-Z. Z. Polym.*, **124**, 83 (1951).
(16) S. Gaumer, Ph.D. Thesis, Michigan State University (1973).
(17) H. K. Yuen, Ph.D. Thesis, Michigan State University (1973).
(18) J. J. Keane and R. S. Stein, *J. Polym. Sci.*, **20**, 327 (1956).
(19) A. E. M. Keijzer, J. J. van Aartsen, and W. Prins, *J. Appl. Phys.*, **36**, 2874 (1965).
(20) E. V. Beebe, R. L. Coalson, and R. H. Marchessault, *J. Polym. Sci., Part C*, **13**, 103 (1966).
(21) G. Wilkes and R. H. Marchessault, *J. Appl. Phys.*, **37**, 3974 (1966).
(22) T. C. Warren and W. Prins, *Macromolecules*, **5**, 506 (1972).
(23) L. G. Shaltyko, A. A. Shepelevskii, and S. ya. Frenkel, *Vysokomol. Soedin., Ser. A*, **12**, 1581 (1970).
(24) G. Ross, *Opt. Acta*, **16**, 611 (1969).
(25) R. Duplessix, C. Picot, and H. Benoit, *J. Polym. Sci., Part B*, **9**, 321 (1971).
(26) Should the short-range correlation function be taken as represented by $F1 = \exp(-\rho/a_1)$, although the data fit much better with the power spectrum of $F2 = \exp(-\rho^2/a_1^2)$, a_1 would even be smaller, being 1200 Å.
(27) D. W. Van Krevelen and P. J. Hoftyzer, "Properties of Polymers Correlations with Chemical Structure," Elsevier, New York, N. Y., 1972.
(28) R. H. Boundy and R. F. Boyer, "Styrene, Its Polymers, Copolymers and Derivatives," Reinhold, New York, N. Y., 1952.